Renewable Energy 239 (2025) 122106

Contents lists available at ScienceDirect

Renewable Energy

journal homepage: www.elsevier.com/locate/renene

Batch rolling-bed dryer applicability for drying biomass prior to torrefaction

Szymon Szufa [a,f,**], Hilal Unyay [a], Zdzislaw Pakowski [a], Piotr Piersa [a], Krzysztof Siczek [b], Mirosław Kabaciński [c], Szymon Sobek [d], Kevin Moj [e], Blaž Likozar [f], Andrii Kostyniuk [f,*], Robert Junga [c]

[a] Faculty of Process and Environmental Engineering, Lodz University of Technology, Wolczanska 213, 90-924, Lodz, Poland
[b] Department of Vehicles and Fundamentals of Machine Design, Lodz University of Technology, 90-537, Lodz, Poland
[c] Department of Thermal Engineering and Industrial Facilities, Opole University of Technology, 5 Mikołajczyka St, 45-271, Opole, Poland
[d] Department of Heating, Ventilation, and Dust Removal Technology, Silesian University of Technology, 20 Konarskiego St, 44-100, Gliwice, Poland
[e] Faculty of Mechanical Engineering, Opole University of Technology, 5 Mikołajczyka St, 45-271, Opole, Poland
[f] Department of Catalysis and Chemical Reaction Engineering, National Institute of Chemistry, Hajdrihova 19, 1001, Ljubljana, Slovenia

ARTICLE INFO

Keywords:
Rolling bed dryer
Wood chips
Dryer modeling
Torrefaction

ABSTRACT

This study investigates the suitability of a pilot-scale batch rolling-bed dryer for drying pine wood chips intended for torrefaction. The batch rolling bed dryer emerges as an ideal solution for further processes like torrefaction, offering a compact design and a wide range of operational parameters. Compared to rotary dryers, it occupies less volume, providing greater efficiency. Additionally, its adjustable drying airflow and compatibility with various biomass forms and particle sizes enhance its versatility. The volumetric evaporation rate was found 13.9 kg/m^3 per hour for the total dryer volume and 78.8 kg/m^3 for the bed volume. Mechanical tests demonstrate satisfactory operation, with potential for further optimization through impeller blade design improvements. The study also presents a simple model using the CDC modeling approach, successfully describing drying curves in most experiments, albeit with some limitations in temperature curve simulations. Overall, the rolling bed dryer proves to be a convenient solution for drying wood chips as a pretreatment for steam torrefaction, offering ease of operation and promising potential for application in continuous torrefaction lines.

1. Introduction

As fossil fuels rapidly deplete and their costs rise, the emphasis on researching alternative, sustainable energy sources grows. This pursuit is essential to address environmental concerns and meet the increasing global energy demand effectively. Finding cost-effective solutions with minimal environmental impact is crucial for long-term sustainability [1]. Biomass, standing as the fourth most significant energy source globally after coal, oil, and natural gas, emerges as a crucial and easily obtainable form of renewable energy within our contemporary energy framework [2]. What sets biomass apart is its nearly carbon-neutral attributes and its widespread natural abundance. This unique combination endows biomass with the potential to make substantial strides in reducing our dependence on fossil fuels and curbing environmental pollution, particularly in terms of mitigating the ominous specter of greenhouse gas emissions [3]. Biomass, in its intricate composition, reveals a diverse makeup, encompassing approximately 40–60 % cellulose, 15–30 % hemicellulose, and 10–25 % lignin, complemented by inorganic minerals and organic extractives [4]. Despite its richness in components, biomass encounters inherent limitations when compared to coal, exhibiting a heterogeneous nature, lower calorific value, higher moisture content, hydrophilic properties, poor grindability, and challenges related to handling, storage, and a lower energy density compared to fossil fuels [5]. These factors collectively impact the feasibility of biomass as a comprehensive alternative to traditional energy sources. Moreover, the combustion of biomass often proves to be

* Corresponding author.
** Corresponding author. Faculty of Process and Environmental Engineering, Lodz University of Technology, Wolczanska 213, 90-924, Lodz, Poland.
E-mail addresses: szymon.szufa@p.lodz.pl (S. Szufa), hilal.unyay@dokt.p.lodz.pl (H. Unyay), zdzislaw.pakowski@p.lodz.pl (Z. Pakowski), piotr.piersa@p.lodz.pl (P. Piersa), krzysztof.siczek@p.lodz.pl (K. Siczek), m.kabacinski@po.edu.pl (M. Kabaciński), szymon.sobek@polsl.pl (S. Sobek), k.moj@po.edu.pl (K. Moj), blaz.likozar@ki.si (B. Likozar), andrii.kostyniuk@ki.si (A. Kostyniuk), r.junga@po.edu.pl (R. Junga).

https://doi.org/10.1016/j.renene.2024.122106
Received 29 April 2024; Received in revised form 25 November 2024; Accepted 5 December 2024
Available online 6 December 2024

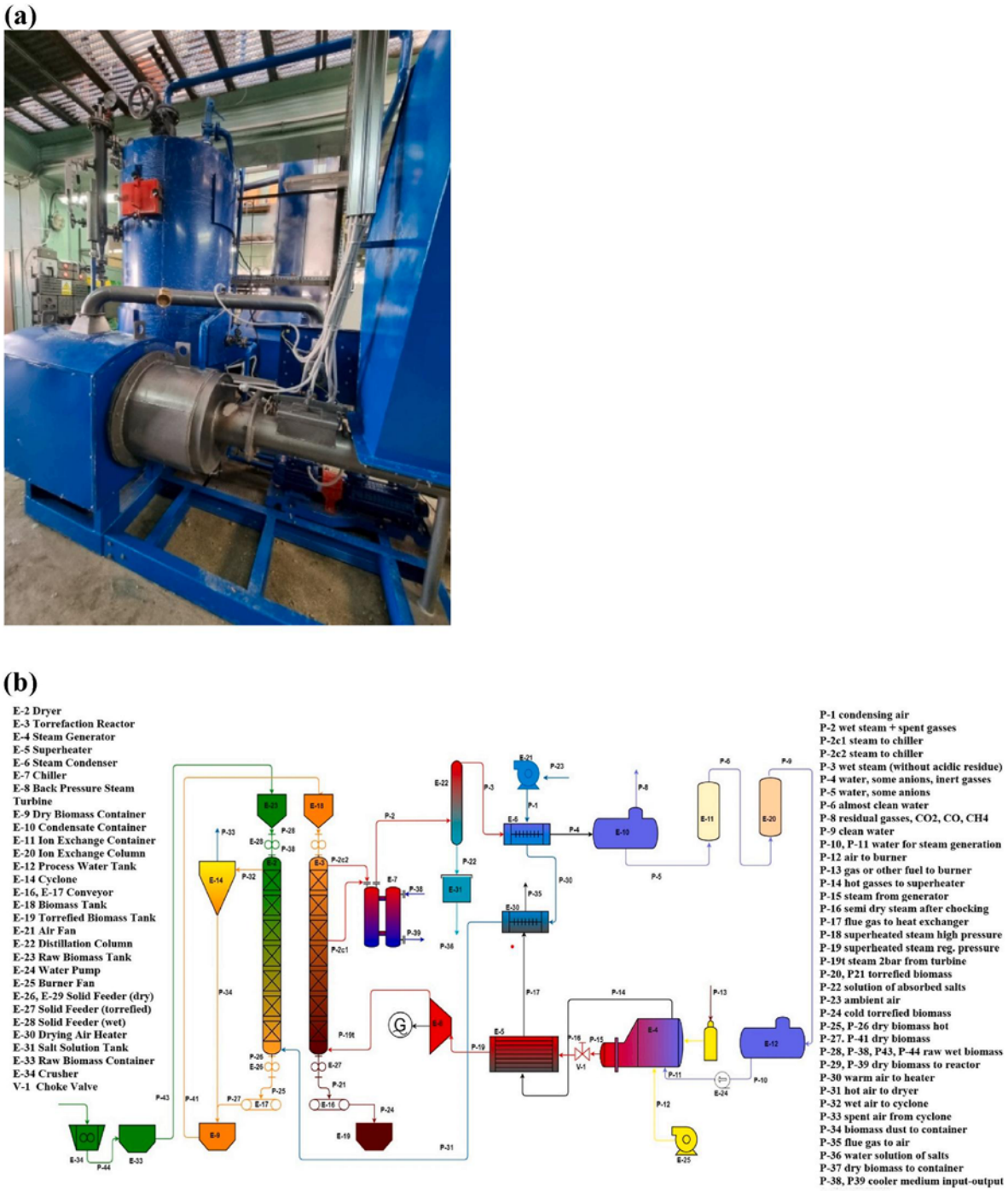

Fig. 1. (a) – Installation for the torrefaction process using SHS in a counter-flow reactor and a rolling bed dryer. (b) – An overall flow diagram of the SHS torrefaction process [9].

inefficient and costly. Consequently, thermal conversion processes such as torrefaction, pyrolysis, hydrothermal liquefaction, gasification, and combustion emerge as imperative solutions to surmount these limitations and elevate biomass into the realm of high-density biofuels. Torrefaction, a form of mild pyrolysis, emerges as a significant eco-friendly thermochemical method for generating solid biofuel [6]. This process enhances the heating value and hydrophobicity, resulting in the production of biochar or hydrochar from a variety of biomass sources, including woody and non-woody residues, agricultural by-products, agro-industrial waste, and municipal solid waste [2].

In small torrefaction reactors with stationary beds operated in countercurrent, the upper section of the bed usually serves as the drying section. However, it is more efficient to pre-dry the biomass prior to torrefaction in a separate apparatus. There are a number of dryer types that can be used for drying biomass: fixed bed (silo), moving bed, fluidized bed, rotary, and recently rolling-bed dryers. Among the advantages of continuous rolling-bed dryers, one can name the following.

- They use less volume than their major competitor - rotary dryers since the rolling bed takes up to 40 % of the total dryer volume, while in rotary dryers, the bed takes only up to 15 %,

- Drying airflow can be adjusted as needed, below the minimum fluidization velocity - it is not so in fluid-bed dryers unless they are vibrated,
- They are impartial to various forms of biomass: chips, flakes, strands, etc.
- They can handle feed with a wide range of particle sizes.

When used in a batch operation, they successfully replace silo dryers and fluid-bed dryers.

This work describes a study on the rolling-bed dryer suitability for drying pine wood chips destined for torrefaction. This research assesses the appropriateness of employing a pilot-scale rolling-bed dryer to desiccate pine wood chips earmarked for torrefaction. The novelty of the rolling bed dryer lies in its pioneering application, as it has not been utilized previously. This innovation represents a breakthrough in drying technology, offering unique advantages for various applications such as torrefaction. Offering a compact design that enhances convenience and encompasses a wide range of operational parameters. Moreover, increasing the biomass fill enhances the evaporation rate per dryer volume, further highlighting its innovative features and potential applications.

1.1. Drying process for torrefaction

1.1.1. The role of drying in the torrefaction line

The drying process is the most energy-consuming stage of biomass torrefaction preceding stages. It is also crucial due to the fact that it is a determinant of the final torrefaction product quality and is also responsible for the smooth operation of the biomass torrefaction line. Several different types of dryers can be used in the biomass torrefaction process.

The drying process is one of the stages in torrefaction technology that consumes the most energy in biomass black pellet production biorefinery plants. Because of this fact, it is crucial that the process occurs as efficiently as possible from an energy point of view by optimizing the energy sources (use energy from the steam condensation as in our proposed installation of Fig. 1) and, subsequently, by lowering the associated energy costs of the heat sources, for both drying and torrefaction itself. From the energy point of view, dryers can use various forms of energy; the most common industry options are woody biomass (wood chips) and natural gas. It is very common for large biomass pellet plants to resort to biomass combustion systems which provide heat to the drying process. This kind of solution is essentially a result of two factors. First of all, due to the economic option, because drying is an energy-intensive consumer, the energy costs are very high, and biomass, in the form of residual forest biomass or even in the form of wastes from the peeler, is always less costly and is usually in abundance. Second, due to the location chosen for the biomass torrefaction biorefinery unit, which should be close to the sources of substrate/raw material, especially if they are away from the natural gas networks.

Production of torrefied biomass together with superheated steam is generally the case in paper mills (lignocellulose as raw material and a large amount of thermal energy waste in the form of superheated steam) or wood processing plants (e.g., companies producing wooden windows - Poland is the leader in this field, having considerable amounts of woody biomass waste - most often pine and large amounts of waste heat that can be used for drying and torrefaction purposes) [7,8]. The drying process consumes the biggest amount of energy in the overall torrefaction process as valorization technology to carbonized solid fuels. Precise control of the pressure and temperature of air for drying biomass and superheated steam for torrefaction allows the overall biomass torrefaction process to be carried out in an economically viable way Additionally, the main innovative idea behind this solution is that the steam after the torrefaction process is condensed, and the conversion heat is used to preheat hot air for the biomass drying process (Fig. 1).

Wood chips, straw, corn stover etc., are various forms of biomass characterized by various levels of moisture content (MC). The drying process of these biomass forms improves their ability to be used as fuel. The water content of residual and waste wood can reach up to 50 wt%, and while biomass with moisture levels of 55–65 wt% can still sustain combustion, the optimum moisture content is 10–15 wt% [7,10]. Their energetic effectiveness is also adversely affected by their inhomogeneity and variable quality [11].

Drying biomass enhances the fuel calorific value the combustion efficiency and can lower emissions [12]. Therefore, for example, it is desirable to lower the moisture content of sawdust [13]. This positive effect of drying biomass was also pointed out by other researches [14]. The raw biomass properties, including water content, bulk density, and particle size distribution, affect the drying kinetics and the dryer energy demand [15]. The positive environmental effect resulting from biomass drying was also reported [16].

The choice of a suitable drying system and drying conditions provides the way to achieve the needed final MC [17]. Various techniques and dryer types are used for the drying process, particularly for various types of biomass. Yi et al. [18] described conventional dryers for biomass, including rotary dryers, fluidized bed dryers, pneumatic dryers, agitated drum dryers, and fixed or moving bed dryers. Solar drying, microwave drying, and far-infrared drying are solely applicable in laboratory and pilot-plant scales. To lower the energy consumption of the drying system, multistage drying, heat recuperation and process integration can be applied.

Conveyor dryers, rotary dryers of single or multiple passes, fixed and moving bed dryers, perforated floor bin dryers, direct and indirect fired rotary dryers, cascade dryers, superheated steam dryers, microwave dryers, fluidized bed dryers, screw-conveyor dryers, and flash or pneumatic dryers can be used for drying biomass depending on particle size and production scale [14,19].

The strategy of integrating waste heat from various sources for the drying process was reported by Alamia et al. [20]. Depending on the form of the waste heat carrier two main types of dryers, differing in how heat is applied to the dried material, can be used - direct or indirect [21]. In direct dryers, heat from the hot medium (air, flue gas, or superheated steam) is directly transferred to the material by convection [22]. In indirect (or contact) dryers, heat is transferred to the dried material mainly by conduction via a heat-transfer surface heated by steam or hot water [23].

The application of various types of dryers in biomass torrefaction lines was described by Brammer and Bridgwater [24]. Nhuchhen et al. [25] described a laboratory-scale torrefaction line with a rotary dryer. Manouchehrinejad and Mani [26] presented the simulation results of an industrial-scale torrefaction line with a direct rotary dryer. Progress in torrefaction lines with separate biomass dryers was described by Chen et al. [27].

The direct dryers also include the rolling bed dryers. The principle of operation of the rolling-bed dryers consists of blowing the hot air through a bed of particles located on the bottom of a stationary horizontal drum through perforations while the bed is slowly mixed by paddles connected to a horizontal impeller shaft. So far, no research describing the application of a rolling-bed dryer in a torrefaction line has been detected, although several companies offer solutions for such dryers for biomass. Rolling bed dryers are handy in various industries, including agriculture, food and chemical processing, pharmaceuticals, biomass and biofuels, and more. Such a drying technology exhibits energy efficiency, cost-effectiveness, and the ability to process various materials [28]. The global demand for rolling-bed dryer market grew at a Compound Annual Growth Rate (CAGR) of 4.80 % between 2023 and 2030 [28]. Rolling-bed dryers can operate in a continuous or batch mode, and the heat may be supplied directly and/or indirectly.

According to Allgaier Process Technology GmbH, in their rolling bed dryer, a large biomass content is permanently circulated and mixed by highly effective paddles [29]. This concept links a flow of large bulks of product with good heat transfer and continuous movement of the

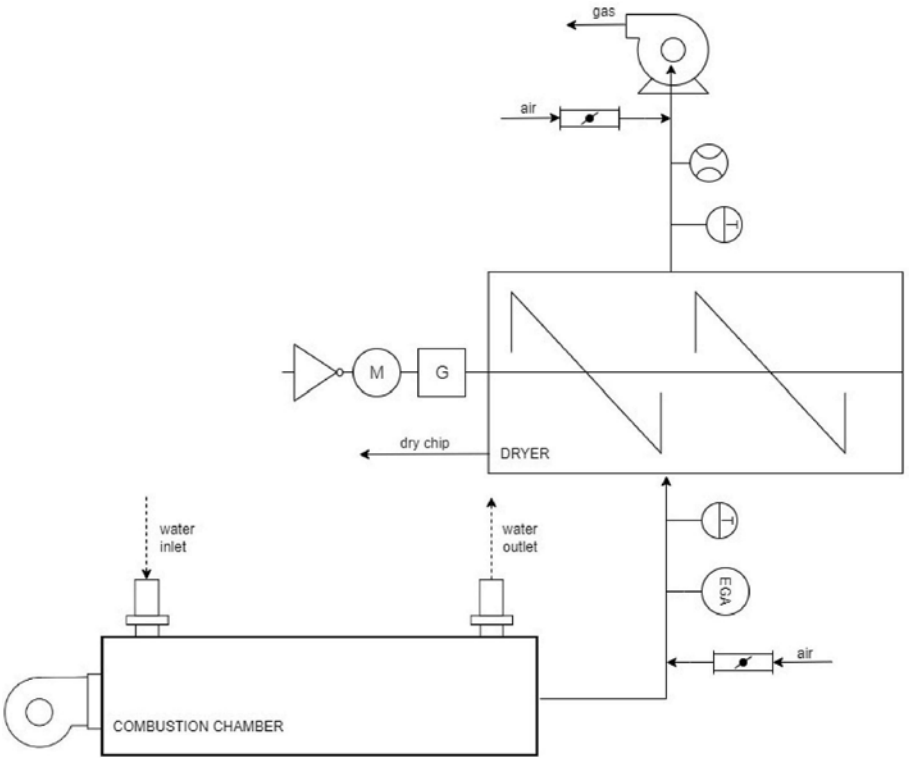

Fig. 2. P&ID of the rolling bed dryer test setup.

Fig. 3. Photographs of the dryer during testing and of the drying chamber.

Table 1
Selected parameters of the experimental runs.

Run	Gas inlet temp.	Gas inlet abs. humidity	Gas superficial velocity	Initial solid MC
	°C	kg/kg	m/s	% w.b.
1	156	0.016	0.146	41.15
2	153	0.017	0.171	35.6
3	156	0.015	0.185	33.55
4	179	0.016	0.177	36.2
5	187	0.019	0.122	38.15
6	187	0.019	0.122	37.65
7	188	0.021	0.121	41.6
8	198	0.019	0.157	37.3
9	198	0.018	0.185	38.9
10	229	0.023	0.132	38.1

product to provide even drying. The drying air is supplied via a perforated plate, on top of which the bulk of the product is moved. The amount of ventilation controls the separation level of fine materials, including dust, fibers, and sand from the bulk material, and the collection of this separately, alongside the actual drying process. The product cleaning parallel with drying allows for enhancing the calorific value of the residual biomass and lowering the ash content. The concept allows using residual energy in a wide range of applications – especially low-temperature waste heat between 80 or 100 °C and about 160–180 °C. Utilizing commercially available standard components the concept dryer can be applied to the pelletizing/briquetting as well as for gasification or torrefaction of biomass. The Allgaier rolling bed dryer eliminates the disadvantages of other conventional dryer types, such as belt dryers, drum dryers, or fluidized bed dryers. It also provides the trouble-less operation even with difficult or large grain sizes, or grain sizes with a tendency to cause jams. Additionally, it allows for good mixing of the bulk product and even residual moisture and cleaning effect for optimum product qualities. It also can use various kinds of residual energy. According to Trojosky and Weiss [30], Allgaier Process Technology developed the rolling bed dryer WB-T with a 25 t/h capacity, combining the advantages of drum dryers and fluidized bed dryers and providing gentle drying at low temperatures. Such a dryer offers high energy efficiency homogeneous and thorough drying of many organic residues. It effectively uses low-temperature exhaust air and has an adjustable velocity of the drying air to process different types of waste. Low product temperatures lead to low emissions and pollution

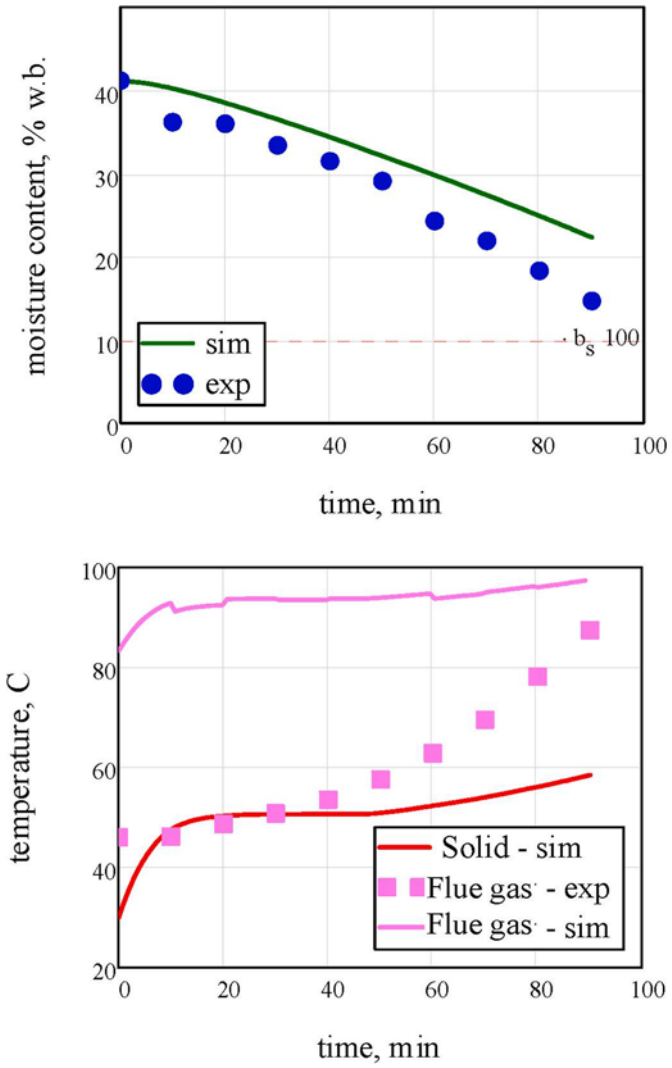

Fig. 4. Drying and temperature curves for run #1. Drying curve fit: $R^2 = 0.981$.

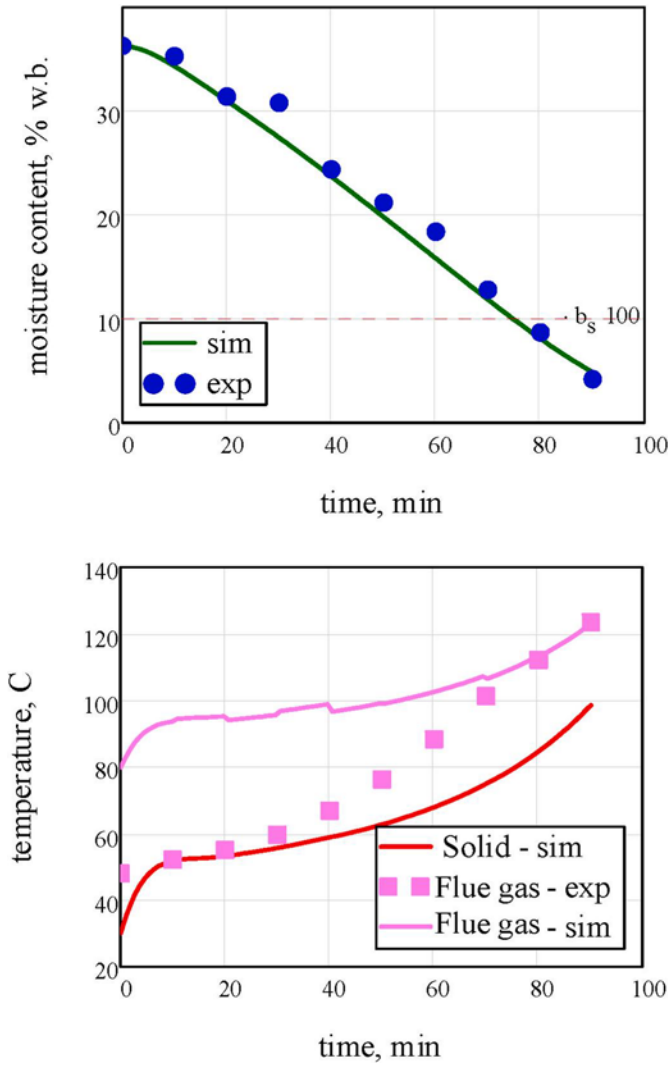

Fig. 5. Drying and temperature curves for run #2.
Drying curve fit: $R^2 = 0.976$.

by total organic compounds. The simple design allows a long residence time and a very homogeneous product drying. The authors reported that using such a dryer for the wet input material with 42 % residual moisture (inhomogeneous material) with a bulk density of 160 kg/m^3 was converted to dry product with a residual MC of 4 % and a bulk density of 99.5 kg/m^3.

ALMO Process Technology developed a new rolling bed dryer, overcoming the issues met in rotary dryers, belt driers, or fluid bed dryers, such as insufficient product residence times, partial overheating of the solid, inability to use low-temperature secondary heat and poor solid mixing [31]. The dryer provided steady and homogeneous mixing of the non-uniform bulk material that stayed in the dryer for long retention times. Such a dryer was installed at Topell Energy in The Netherlands. Topell used two such dryers to convert wood waste into charcoal by torrefaction. Such a dryer can produce fuels by preparing and drying organic wastes such as wood chips safely, environmentally friendly, and economically.

1.1.2. Modelling of the drying process principles

To effectively describe the drying process, one needs to know its kinetics, i.e., the dependence of material MC and temperature on time. For this, usually, a small batch of the raw material is dried in laboratory conditions, as close to the industrial ones as possible. Such experimental studies focusing on biomass drying kinetics mechanism and the characteristics of dried products have been performed [32–34]. However, conducting full-scale experiments for various products and types of dryers either involves high costs or is impossible because of various economic and organizational reasons [35].

On the other hand, mathematical modeling of the drying process enables the simulation and design of dryers for specified working conditions at a fraction of the cost [36]. The mathematical model of a dryer consists of balance equations of heat and mass for each phase, kinetic equations that govern heat and mass exchange between phases, thermodynamic properties of all phases, and geometrical relationships describing the dryer. For a batch dryer, the mathematical model of the process includes a system of differential and/or integral equations binding input and output quantities as well as control parameters of the drying process, that can also be represented using algebraic equations and inequalities, which sometimes also act as boundary and initial conditions. Sometimes, logical rules are also introduced into the mathematical model. The solution of the system of equations should make it possible to predict the process parameters as a function of time anywhere in the dryer based on the initial and boundary conditions, c.f [37, 38]. Therefore, the use of various simulation models allows for predicting the course of the drying process [39].

In these models, it is crucial to know the rate at which moisture leaves the solid phase, the drying rate, defined as:

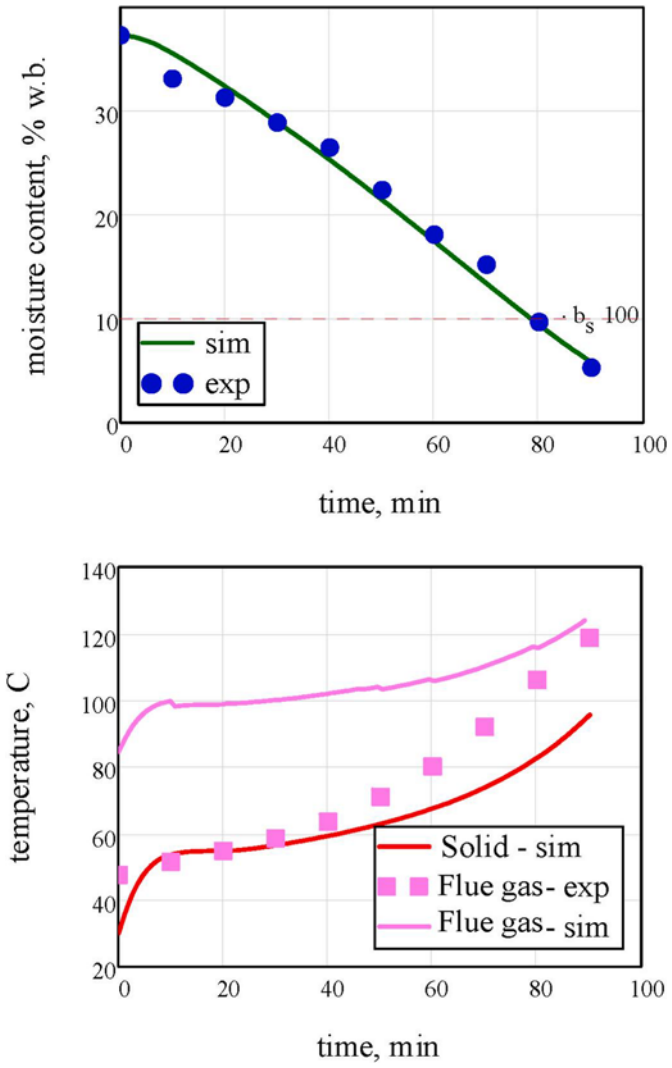

Fig. 6. Drying and temperature curves for run #3. Drying curve fit: $R^2 = 0.962$.

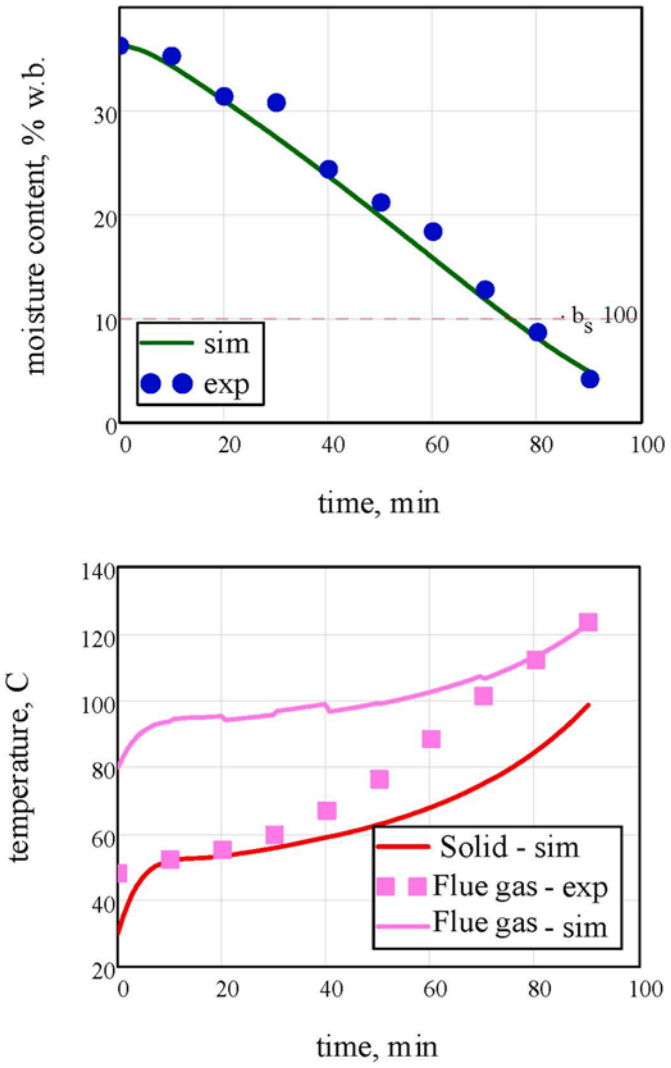

Fig. 7. Drying and temperature curves for run #4. Drying curve fit: $R^2 = 0.895$.

$$w_D = -\frac{m_S}{A_p}\frac{dX}{d\tau} \quad (1)$$

Most solids, including biomass, contain both free and bound moisture. Free moisture evaporates according to the rules of convective heat and mass transfer. On the other hand, complex mechanisms of bound moisture evaporation involve capillary flow of liquid and vapor phases, desorption and diffusion of water vapor and are difficult to describe mathematically. To simplify the problem empirical or semiempirical models are used. The most rigorous of them is the diffusion equation with empirically determined moisture diffusivity. The other three involve the characteristic drying curve (CDC), thin layer equations (TLE), and reaction engineering approach (REA).

The diffusion equation approach requires solving a 2nd order partial differential equation of diffusion (Fick's second law), which is feasible for isometric, preferably spherical particles, but not recommended for nonisometric particles such as wood chips or similar. The TLE approach is mainly used in deep bed drying of grains and other agricultural granular solids. The TLE has the form $X = f(\tau)$, of which the simplest is the equation of Page [40]. Numerous others were also proposed for various materials [41,42]. In the CDC approach the drying rate of bound moisture is related to the drying rate of free moisture by a simple equation. Details of this approach will be presented in the Evaluation of Experimental Results section 4 of this work.

Mohd Yusof et al. [16] work is an example of the REA, where the apparent activation energy of the material is established and related to its MC during drying. In this approach, the normalized activation energies can be described by a single equation independent of the drying conditions and dryer types. Recently, it is become attractive to use various artificial intelligence methods, including genetic algorithms and neural networks. Such methods are used to model drying curve characteristics [41,43] dynamically. They, however, require the use of specialized software.

1.1.3. *Modelling of biomass drying*

Several mathematical modeling studies on biomass drying allowed for predicting drying behavior, diffusivity, the temperature profile of biomass, and VOCs emissions that occurred while drying [40,44,45]. The diffusion-based models were used to describe the drying kinetics of biomass [46]. Such models were governed by the diffusivity describing the migration of moisture and vapor in the solid phase. The determination of a diffusivity relationship between temperature and MC needed a large number of tests. Gebreegziabher et al. [46] elaborated a mathematical model comprising material and energy balances, heat transfer, and drying kinetics for determining the optimum drying conditions of biomass. Drying kinetics based upon Fick's second law of diffusion allowed for the determination of the energy and capital expenditures for the drying process. He and Wang [47] elaborated a model to simulate moisture diffusion in Birch during the drying process. A diffusion model

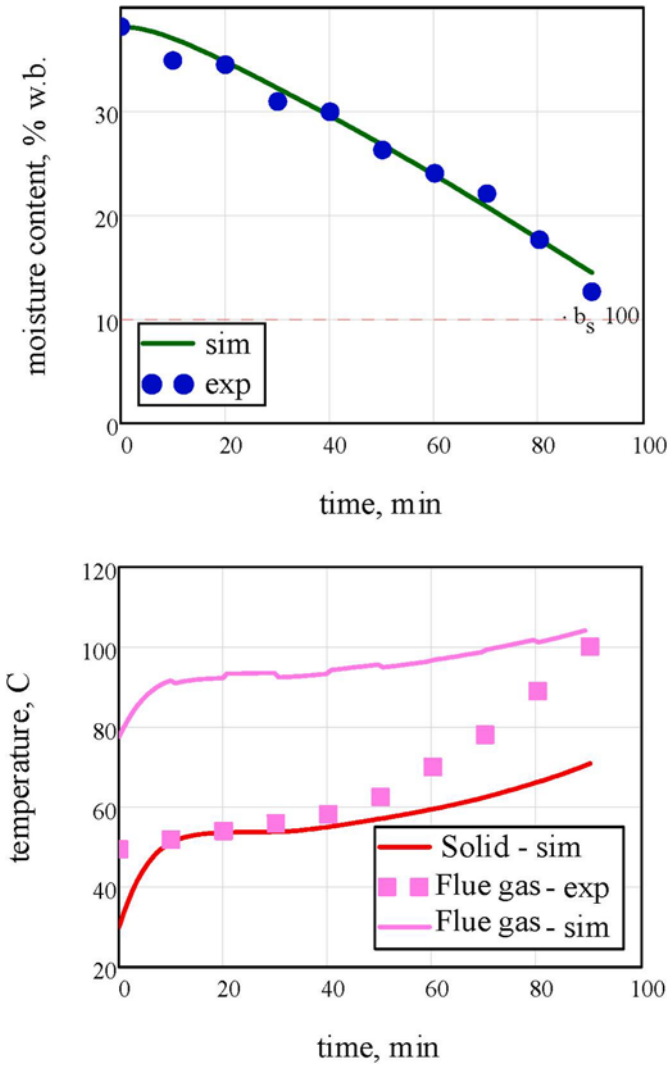

Fig. 8. Drying and temperature curves for run #5. Drying curve fit: $R^2 = 0.988$.

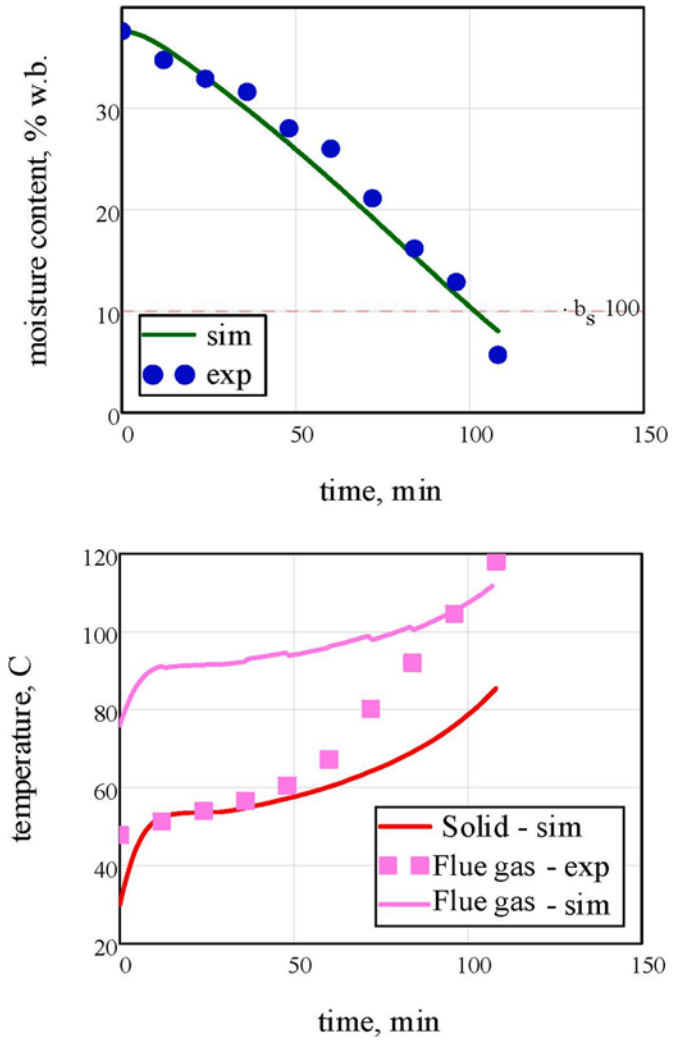

Fig. 9. Drying and temperature curves for run #6.
Drying curve fit: $R^2 = 0.983$.

described the mechanism of moisture variations in Birch samples during the drying process according to Fick's second law. The moisture diffusion coefficients of Birch ranged from 1.2×10^{-7} m^2/h to 9.6×10^{-7} m^2/h with temperatures in the range of 20 °C–60 °C. The diffusion coefficient depended on temperature in accordance with the Arrhenius equation.

Cai and Chen [48] studied the non-isothermal drying kinetics of wheat straw and corn stalks by the thermogravimetric method. The drying behavior of such agricultural products was described using TLE models such as Newton, Henderson, and Pabis, logarithmic, and Page, whose parameters resulted from fitting experimental data obtained. Page's model best described the non-isothermal drying characteristics of agricultural products studied. González et al. [49] elaborated a kinetic model for drying biomass of *Piptocoma discolor*. They analyzed five models of TLE and found that the Aidawati TLE characterized by parameters a = 1.1318, k = 0.0637765, n = 0.560617, and b = −0.193993 was the best. A study on drying kinetics of whole and slashed canes of *Arundo donax* L. [32] used six TLE drying models to fit the experimental drying data, achieving good performance. The logarithmic model showed the best fit.

Xu and Pang [50] elaborated a mathematical model for simulating the drying of the woody biomass as chips in a rotary dryer based on energy and mass balance and transfer, experimental drying kinetics of the wood chips, and using data from the literature for the residence time. The model used by the CDC was obtained experimentally. The model was applied to co-current and countercurrent rotary dryers. Mohd et al. [16] used REA to model the kinetics of the drying process of sawdust conducted using a convective hot air humidity-controlled oven in a laboratory setup. The normalized (relative) activation energy curve generated from one drying experiment was employed to predict the drying kinetics and temperature profiles. The detailed multiscale modeling of biomass drying was also attempted [51], but the modeling was complex and was unfavourable for quick decision-making in industrial operations.

2. Material

The raw material was wood chips of pine (*pinus sylvestris*) obtained in the summer of 2023 from forest clearings near Prószków in the Opole Voivodeship (Poland). The 15–40 mm sieve fraction was selected from the entire batch by sieving. Since each experimental batch used ca. 40 kg of biomass to limit the amount of stored material, it was recycled by rewetting with a necessary mass of water to obtain MC of approximately 35 % w.b. After rewetting and mixing, the material was stored overnight in an airtight container for MC to equalize within particles. The wet chips' bulk density, determined per the standard PN-EN ISO 17828:2016–02, was 394 ± 3.2 kg/m^3 (type An uncertainty). The apparent density was determined based on measurements of mass and volume of 10 selected average chips from the entire batch. Volume measurements were carried out using a Phoenix V Tome xS CT scanner

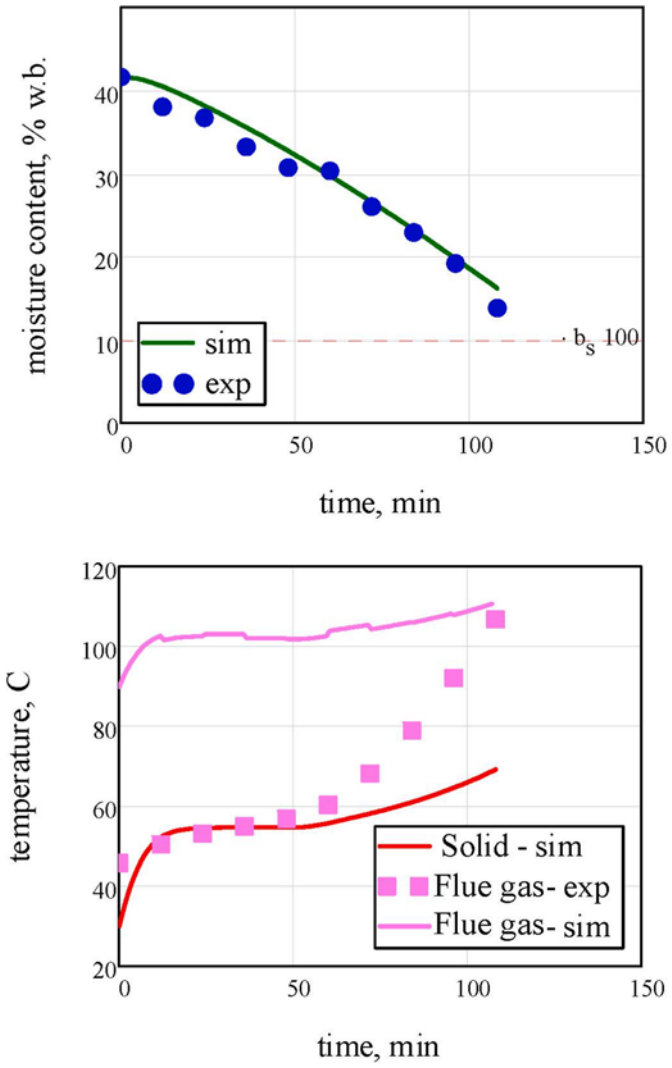

Fig. 10. Drying and temperature curves for run #7. Drying curve fit: $R^2 = 0.713$.

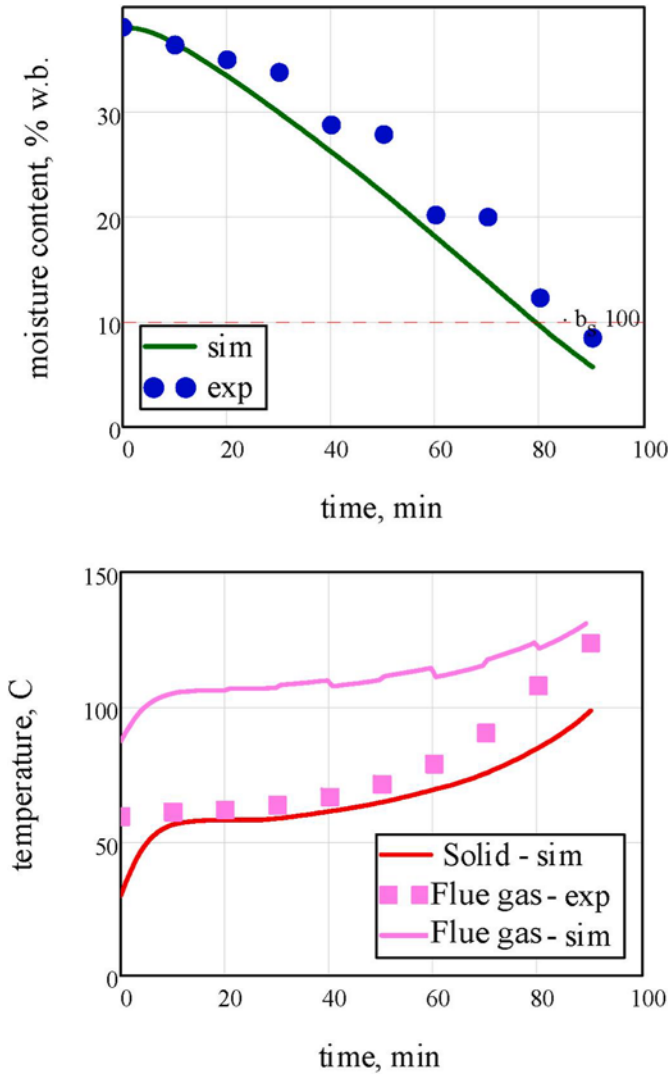

Fig. 11. Drying and temperature curves for run #8. Drying curve fit: $R^2 = 0.669$.

(Waygate Technologies, Germany) with a grayscale detector resolution of 1000 x 1000 pixels and a pixel size of 200 μm, a rotary table, and a microfocus X-ray tube with a maximum accelerating voltage of 240 kV. An exemplary scan processed in VG Studio software is presented in the Support Information file (Fig. S1). The average wet chips' apparent density was 806 kg/m^3, with ±71 kg/m^3 measurement uncertainty calculated with a convergence factor (k) of 2, corresponding to a 95 % confidence level. Sphericity is the ratio of the surface area of a sphere of the same volume to that of the particle.

$$\psi = \frac{\pi^{1/3}(6V_p)^{2/3}}{A_p} \tag{2}$$

Unfortunately tomographic particle surface areas came out much higher than expected, thus leading to a very small sphericity. All surface defects were probably added to the total surface in tomography, while the flow hydrodynamics indicates that they are covered in the boundary layer and do not participate in heat and mass transfer. Therefore, the actual sphericity was calculated assuming that particles are parallelepipeds 25x10 × 6 mm in size. The heat capacity of wood was taken as linearly dependent on temperature according to Dupont et al. [52]:

$$c_S(t) = 0.001(111 + 3.783T) \tag{3}$$

Sorption isotherm of wood was fitted to the data of Krupinska et al. [53] and has the form

$$\varphi_e = 1 - exp\left[-0.110(39.093 + t)X^{1.068}\right] \tag{4}$$

The above form of the sorption isotherm dependent on temperature allowed for calculation of the isosteric (at constant X) heat of sorption from the Clausius-Clapeyron equation. It varied between ca. 650 kJ/kg at X = 0 and 0 for X ≈ 1.

3. Experimental

Drying experiments were conducted in the Laboratory of Combustion Process Research at the Opole University of Technology (DMS coordinates: 50°39′08.3″N 17°54′08.2″E). The setup comprised a rolling bed-type dryer with a rotor, systems for generating and stabilizing the drying medium temperature, and facilities for removing humid gas. The system's layout is depicted in Fig. 2.

The rotary dryer's primary components include a drying chamber, a rotating shaft equipped with seven specially designed blades, a motor reducer with an engine, and measuring equipment. The cylindrical drying chamber measures 1100 mm in length and 800 mm in diameter. Its body and side covers, made of 1.4301 stainless steel (AISI 304), have 3 mm and 4 mm thicknesses, respectively. A perforated sieve with 2 mm diameter laser-cut holes is mounted at the chamber's bottom. These

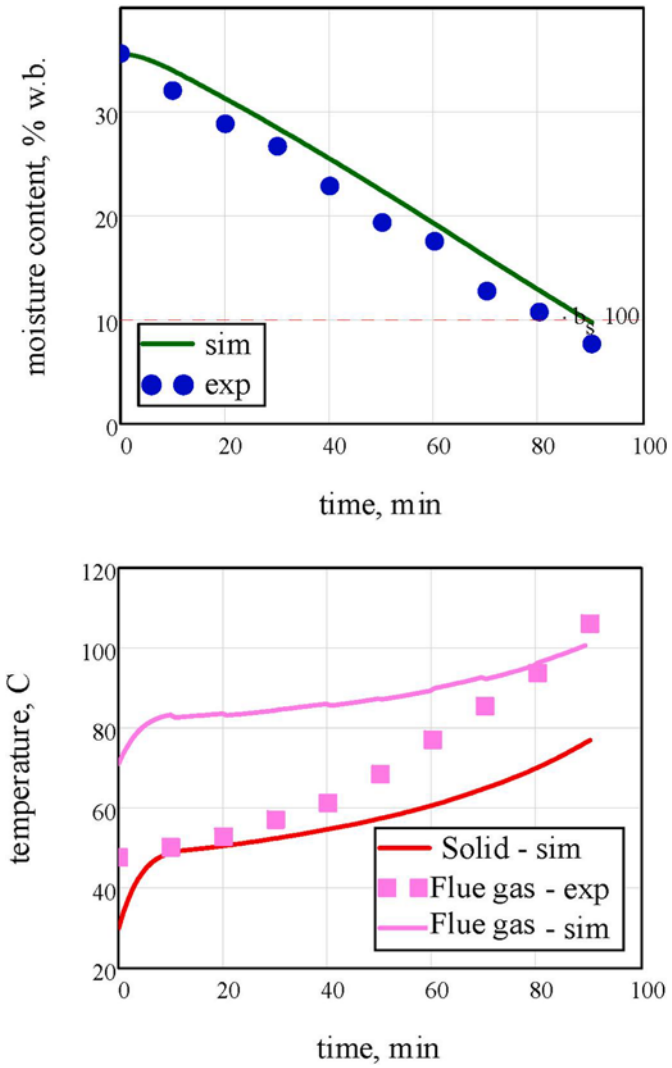

Fig. 12. Drying and temp. curves for run #9. Drying curve fit: $R^2 = 0.929$.

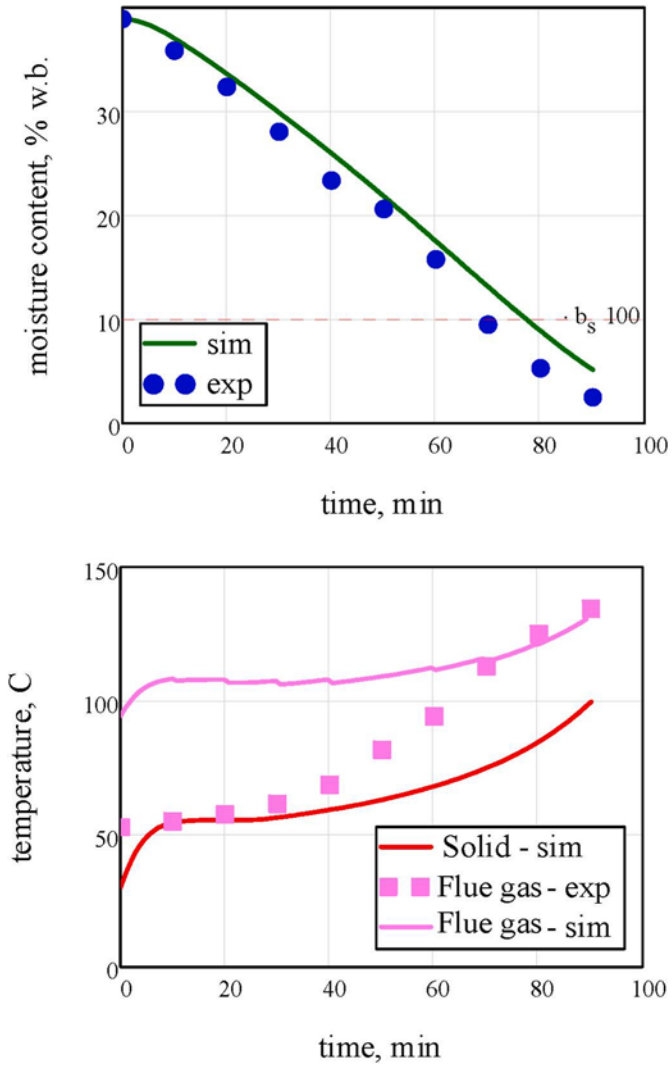

Fig. 13. Drying and temp. curves for run #10.
Drying curve fit: $R^2 = 0.96$.

holes follow a hexagonal pattern, spaced 10 mm apart at the vertices of equilateral triangles, allowing the free surface to constitute 4 % of the total sieve area. The sieve is crafted from a 2 mm thick 1.4301 stainless steel sheet. A worm gear reducer and a three-phase 0.55 kW motor drive the shaft. Mounted on the rotary shaft, the motor reducer's reactive torque is compensated by a reaction arm. A Liteone Eov6000 series frequency inverter is employed to control the shaft's rotational speed, offering an adjustment range of −50 % to +20 % of the nominal value, i.e., 7–16.8 rpm. Fig. 3 shows photographs of the dryer and the drying chamber during experiments.

The hot gas generation system includes a combustion chamber with a water jacket, a Riello Gulliver BGK0.1 oil burner capable of delivering 17–35 kW of power, and a duct fitted with a damper for external air intake. The combustion chamber is part of a water supply temperature stabilization system described in detail in Ref. [42]. The post-drying gas exhaust passes through a duct system with an external air bypass and a regulatory damper installed before the exhaust fan.

Type K thermoelectric sensors, accurate to $\leq \pm 1.5$ °C and integrated with an APAR multi-channel measurement recorder, measured the gas temperature at the dryer's inlet and outlet. This setup enabled online system monitoring with 1-s intervals. Additionally, a TESTO 330-2 LX analyzer was mounted on the inlet drying gas duct to measure the gas composition and determine its absolute humidity. In the velocity measurements, a standardized Pitot tube of 110 mm length was used, equipped with a SIEMENS SITRANS P pressure transducer with a measuring range of 1–60 mbar, a sensitivity of 1 Pa, and an accuracy of <0.065·r (%), where r represents the nominal measuring range. Before performing the drying tests, a number of preliminary runs were carried out to determine the operability range of the setup. As a result of preliminary tests, it turned out that the key factors for the proper operation of the drying system were the quality of the feed, in particular length of particles. Wood chips that had not been fractionated, i.e., containing long and thin branches, jammed between the drum and the rotor blades, blocking the mixing system. The problem was solved by sifting the material, mainly by removing long branches, increasing the distance between the drum and the blades to 20 mm, and changing the angle of inclination of the blades relative to the drum. Despite this, in order to avoid mechanical problems during drying tests, the drum fill ratio was kept low at ca. 18 % of the total volume. Preliminary research also made it possible to determine the optimal rotational speed of the shaft and blade system. In the preliminary tests, the positions of the flaps at the drying gas inlet and the flaps in front of the exhaust fan were also determined in order to stabilize the thermokinetic conditions of the process, mainly the gas inlet temperature and the stream of removed humid gas. Each experimental run followed a predefined procedure. Initially, the hot gas generation system was warmed up to reach and maintain the pre-set temperature at the dryer's inlet, typically taking about 50 min. Upon reaching the desired inlet temperature, the flue gas

evacuation system was activated by adjusting the damper before the fan, thus regulating the entire system's performance. The batch of wood chips was then loaded, and the dryer's rotating shaft was activated and set to a constant value of 10 rpm. Each 120 min experimental run collected material samples every 10 min through an inspection hole for MC analysis. The dried wood chips were collected in airtight glass containers and transported to the Laboratory of Instrumental Analysis in Environmental Engineering and Energy at the Opole University of Technology, where moisture content analysis was performed using the drying method in accordance with EN ISO 18134–1:2023. All samples were analyzed in duplicate to determine the measurement uncertainty.

4. Evaluation of Experimental Results

In order to evaluate the experimental results, a simple theoretical model of a batch drying process in the rolling bed was proposed. The drying rate is the crucial parameter of the model. Green wood contains both unbound moisture above the fiber saturation point and bound moisture below the FSP. When removing the unbound moisture, the drying rate can be calculated on the basis of the external driving force as

$$w_{DI} = k_Y[Y_e(t_m, X) - Y] \tag{5}$$

where Y_e is the equilibrium humidity on the particle surface, and Y is the humidity of the surrounding air. The driving force in the bound moisture removal period is the MC gradient inside the particle. To calculate the drying rate a solution of moisture diffusion equation in a complex particle geometry is needed. To avoid this, by assuming that a single wood particle is a lumped-parameter object, its drying rate, in the period where drying is controlled internally, can be described by the characteristic drying curve (CDC) proposed by Keey and Suzuki (1974) [54]. The CDC describes the dependence of the ratio f of the actual drying rate to the drying rate in the free-moisture evaporation period vs. the dimensionless moisture content Φ. It is a property of the material itself: its particle size, sphericity, and internal moisture diffusivity. In this work, the following CDC equation of Filonenko, 1939 with parameters obtained by Krupińska [55], was used:

$$f(\Phi) \stackrel{\text{def}}{=} \frac{w_D}{w_{DI}} = \frac{\Phi^{0.65}}{\frac{1.35}{(X_{cr}-X_e)^{0.65}} - 0.26\,\Phi^{0.65}} \tag{6}$$

$$\text{where } \Phi = \frac{X - X_e}{X_{cr} - X_e} \tag{7}$$

The bed is assumed to be perfectly mixed due to the continuous mixing of the bed by the built-in horizontal paddled impeller. It continuously exchanges heat and moisture with diluted flue gas entering the perforated drum bottom and flowing upwards through the bed. The flow of gas is assumed to correspond to the plug-flow conditions.

Since the vertical cross-section of the bed is semicircular, the velocity of the vertical gas flow is distributed across the bed width. It is greater at the periphery, where the bed is thinner, and smaller in the center, where the bed is the thickest. In order to simplify the model and make it one-dimensional, it is assumed that the bed has the form of a slab. The height of the slab is an arithmetic mean of the actual bed height and the height of the perforated bottom measured in the center of the drum. The width of the slab is calculated by dividing the actual area of the bed cross-section by such obtained bed height.

With the above assumptions, the model of the mass and heat exchange of the solid phase and the gas phase flowing upwards is described by the following equations:

$$\frac{dY}{dh} = \frac{BLa_V}{W_B} w_D(h) \tag{8}$$

$$\frac{dt_g}{dh} = \frac{BLa_V}{W_B} \frac{(\alpha + c_A w_D(h))(t_g(h) - t_m)}{c_H(t_g(h), Y(h))} \tag{9}$$

These equations are solved numerically at a given time with the following boundary conditions:

$$\text{tg}(0) = \text{tgin}\ \text{Y}(0) = \text{Yin} \tag{10}$$

Based on the obtained solutions, the integral mean fluxes of mass and heat exchanged by the gas and the bed are calculated:

$$w_D = \frac{1}{H}\int_0^H w_D(h)dh \tag{11}$$

$$q = \frac{1}{H}\int_0^H q(h)dh \tag{12}$$

They are used in the following kinetic equations for the bed moisture and temperature:

$$\frac{dX}{d\tau} = -\frac{BLHa_V}{m_S} w_D \tag{13}$$

$$\frac{dt_m}{d\tau} = \frac{1}{c_S + c_{Al}X} \frac{BLHa_V}{m_S} \{q + w_D[(c_{Al} - c_A)t_m - \Delta h_{v0} - \Delta h_s]\} \tag{14}$$

with the following initial conditions:

$$\text{t}_\text{m}(0) = \text{t}_\text{m0}\ \text{X}(0) = \text{X}_0 \tag{15}$$

Local heat and mass transfer rates between the gas phase and the bed are calculated as:

$$q(h) = \alpha(t_g(h) - t_m) \tag{16}$$

$$w_D(h) = k_Y[Y_e(t_m, X) - Y(h)]f(X) \tag{17}$$

The heat and mass transfer coefficients in these equations have been the subject of many research works. A number of papers presented correlations for packed beds of spheres, cylinders, and other particles of well-defined geometry [56]. However, for isometric particles of irregular shape, only a few correlations exist, where the irregularity of shape is represented by the particle sphericity ψ. This work calculated the heat transfer coefficients from the following correlations [57].

$$Nu_p = 2.269\, Re_p^{0.49}\, Pr^{0.33}(1-\varepsilon)^{0.51}\psi \text{ for } \frac{Re_p}{6(1-\varepsilon)} \le 50 \tag{18}$$

$$Nu_p = 1.272\, Re_p^{0.59}\, Pr^{0.33}(1-\varepsilon)^{0.41}\psi \text{ for } \frac{Re_p}{6(1-\varepsilon)} > 50 \tag{19}$$

Mass transfer coefficients are usually calculated from the so-called "heat and mass transfer analogies", typically that of Chilton and Colburn. However, in the Lewis analogy, commonly used in drying, the mass transfer coefficient k_Y is simply obtained by dividing the heat transfer coefficient by the humid heat capacity of the gas phase. For simulation purposes, the following mean properties of the particles were taken: $d_p = 14$ mm, $\psi = 0.689$, $\rho_p = 603$ kg/m^3, $\rho_b = 392$ kg/m^3.

The gas phase was a diluted flue gas from an oil-burning heater. Its composition was measured in each run, and its volumetric percent contents of O_2, CO_2, H_2O, and N_2 were recorded together with its temperature. On this basis the inlet gas phase absolute humidity was calculated. Since gas composition only slightly differed from air its physical properties (dry heat capacity, density, viscosity, heat conductivity) were taken as for air.

Since the inlet gas temperature varied insignificantly with time, the average mean temperature was assumed constant during each measurement. However, the actual mass and bed dimensions were corrected to account for samples taken every 10 min to measure the bed MC in duplicate. The mass of each sample was ca. 1.1 kg.

The actual tests were carried out trying to maintain a relatively equal initial MC, around max. 40 %, which corresponds to the parameters of waste wood chips from the sawmill industry or forest wood left outdoors for several days to dry. The dryer is designed to operate as part of a

torrefaction system, utilizing flue gases from a biomass-fired boiler as the drying medium for wood chips. Consequently, the test temperatures were chosen to reflect the exhaust gas temperatures from the boiler, ranging from 155 °C to 230 °C. Therefore, the independent variables in the experiments were the inlet temperature of the drying gas, which was assumed to be around 155 °C (3 measurements), 180 °C (1 measurement), 190 °C (3 measurements), 200 °C (1 measurement), and 230 °C (1 measurement) and dynamic pressure behind adjustable diaphragms. The repeated measurements under unchanged process parameters (e.g., measurements 1–3) were used to determine the uncertainty of the conducted experiments. The operational parameters for all 10 experimental series performed are shown in Table 1.

The results of simulations with the above model are shown in Figs. 4–13. The measurement uncertainty for the temperature was ±1.6 °C, considering the accuracy of the thermocouple class and the transmitter. Meanwhile, the maximum uncertainty for the moisture content was ±1.35 %, determined by taking into account both type An uncertainty, derived from the statistical analysis of MC test results, and type B uncertainty, associated with the precision of the measurement equipment. The R^2 factor represents the quality of fit.

The simulation results show a satisfactory quality of drying curve fit to experimental data. Unfortunately, the quality of temperature curve fit is not yet satisfactory. The experimental exit air temperatures are rather closer to the predicted bed temperatures than the predicted exit air temperatures. To improve this, further simulations should use a 2D model of the bed and account for the variability of bed properties with moisture content. It would also be worthwile to measure the mean particle temperature in the samples taken from the bed for MC determination, for comparison with the simulation results.

As a result of the experiments, it was also noticed that drying was promoted not only by the high temperature of the drying gas (obviously) but also by the high speed of the drying agent in the system, intensifying the removal of humid gas from inside the dryer chamber. Regarding the experimental drying profiles, the rolling bed performs well in both unbound and bound moisture ranges. Usually, traditional dryers provide good and relatively rapid unbound moisture evaporation to about 20 w. b.%, after which particle diffusion and stationary bed mass transfer resistances significantly slow down the drying process.

5. Conclusions

Mechanical tests have proven that our rolling bed dryer of 800 mm ID for 15–40 mm wood chips operated satisfactorily at an impeller rpm of 10 and the degree of fill of ca. 18 %. In order to increase the degree of fill to 40 % as planned, more work on the design of the impeller blades is required. It was also observed that the current impeller system is sensitive to the presence of long particles like broken twigs. At the operating conditions of run #1, the volumetric evaporation rate was 13.9 kg/(m^3·h) per total dryer volume and 78.8 kg/(m^3·h) per bed volume. Obviously, increasing the degree of fill would improve the evaporation rate per dryer volume. The proposed simple model using the CDC approach and experimentally measured wood particle properties worked satisfactorily to describe drying curves in the majority of the performed experiments. Simulated temperature curves, more sensitive to parameters, did not yet satisfactorily reproduce the experimental results in all cases. Necessary improvements of the model would require a 2D approach to the bed transversal cross-section and taking care of the variable particle properties.It was shown that the rolling bed dryer is a convenient solution to drying wood chips in a torrefaction system due to its compactness, ease of operation and wide range of operational parameters. Similarly a continuous rolling bed dryer will be a good solution in a continuous torrefaction line.

CRediT authorship contribution statement

Szymon Szufa: Writing – review & editing, Writing – original draft, Visualization, Validation, Supervision, Software, Resources, Project administration, Methodology, Investigation, Funding acquisition, Formal analysis, Data curation, Conceptualization. **Hilal Unyay:** Writing – review & editing, Writing – original draft, Visualization, Validation, Software, Project administration, Methodology, Investigation, Formal analysis, Data curation, Conceptualization. **Zdzislaw Pakowski:** Writing – review & editing, Writing – original draft, Visualization, Investigation, Data curation. **Piotr Piersa:** Writing – review & editing, Investigation, Data curation. **Krzysztof Siczek:** Writing – review & editing, Investigation, Formal analysis, Data curation. **Mirosław Kabaciński:** Writing – review & editing, Investigation, Data curation. **Szymon Sobek:** Investigation, Data curation. **Kevin Moj:** Investigation, Data curation. **Blaž Likozar:** Supervision, Project administration. **Andrii Kostyniuk:** Writing – review & editing, Writing – original draft, Validation, Project administration. **Robert Junga:** Writing – review & editing, Writing – original draft, Investigation, Data curation.

Declaration of competing interest

The authors declare that they have no known competing financial interests or personal relationships that could have appeared to influence the work reported in this paper.

Acknowledgements

The publication was produced as part of the NAWA Mieczysław Bekker program: “BioGainValue - Research on biomass torrefaction process using superheated steam and properties on new bio-based products”. Grant No. BPN/BEK/2021/1/00248/U/DRAFT/00001 and BioTrainValue (BIOmass Valorization via Superheated Steam Torrefaction, Pyrolysis, Gasification Amplified by Multidisciplinary Researchers TRAINing for Multiple Energy and Products’ Added VALUEs), with project number: 101086411, funded under Horizon Europe’s Maria Skłodowska-Curie Staff Exchange program. The authors express their gratitude for the financial support provided by CARBIOW (Carbon Negative Biofuels from Organic Waste) Research and Innovation Action, which is funded by the European Union under the Horizon Europe Programme, under grant agreement ID: 101084443.

Appendix A. Supplementary data

Supplementary data to this article can be found online at https://doi.org/10.1016/j.renene.2024.122106.

Nomenclature

A	- contact area of phases, m
a_v	- contact area of phases per unit volume of the bed = 6(1−ε)/(d−pψ), 1/m
B	- equivalent width of the bed, m
c	- heat capacity, kJ/(kg•K)
c_H	- humid heat capacity of gas phase = $c_B + c_A$Y, kJ/(kg•K)
d_p	- equivalent particle diameter, m
H	- equivalent height of the bed, m
h	- running height, m
Δh_{v0}	- latent heat of vaporization of water, kJ/kg
Δh_s	- isosteric heat of sorption, kJ/kg
k_Y	- mass transfer coefficient gas-solid, kg/(m^2•s)
L	- length of the bed, m
m_S	- mass of the solid in the bed (dry basis), kg
q	- interfacial flux of heat, kW/(m^2•s)
T	- temperature, K
t	- temperature, °C
u_g	- mean superficial gas phase velocity, m/s
w_D	- actual drying rate, kg/(m^2•s)
w_{DI}	- drying rate in the constant-rate period, kg/(m^2 •s)

V - volume
X - moisture content, kg A/kg•S
Y - absolute humidity of gas phase, kg A/kg•B

Greek

α - heat transfer coefficient gas-solid, kW/(m^2•K)
ε - bed voidage (porosity)
λ_g gas phase heat conductivity, kW/(m•K)
ρ_g - gas phase density, kg/m^3
μ_g - gas phase dynamic viscosity, Pa•s
ψ - particle sphericity

Dimensionless

Nu_p - Nusselt number, $\alpha d_p/\lambda_g$
Pr - Prandtl number for gas phase, $c_p\ \mu_g/\lambda_g$
Re_p - particle Reynolds number, $u_g d_p \rho_g/\mu_g$

Subscripts

A - moisture in vapor phase
Al - moisture in liquid phase
B - dry gas
S - dry solid
cr - critical (≈FSP)
e - equilibrium
g - gas phase
in - at inlet
m - material (wet solid)
p - particle

References

[1] C. He, C. Tang, C. Li, J. Yuan, K.Q. Tran, Q.V. Bach, R. Qiu, Y. Yang, Wet torrefaction of biomass for high quality solid fuel production: a review, Renew. Sustain. Energy Rev. 91 (2018) 259–271, https://doi.org/10.1016/j.rser.2018.03.097.

[2] A. Kostyniuk, B. Likozar, Wet torrefaction of biomass waste into value-added liquid product (5-HMF) and high quality solid fuel (hydrochar) in a nitrogen atmosphere, Renew. Energy 226 (2024) 120450, https://doi.org/10.1016/j.renene.2024.120450.

[3] P.N.Y. Yek, Y.W. Cheng, R.K. Liew, W.A. Wan Mahari, H.C. Ong, W.H. Chen, W. Peng, Y.K. Park, C. Sonne, S.H. Kong, M. Tabatabaei, M. Aghbashlo, S.S. Lam, Progress in the torrefaction technology for upgrading oil palm wastes to energy-dense biochar: a review, Renew. Sustain. Energy Rev. 151 (2021) 111645, https://doi.org/10.1016/j.rser.2021.111645.

[4] A. Kostyniuk, B. Likozar, Catalytic wet torrefaction of biomass waste into bio-ethanol, levulinic acid, and high quality solid fuel, Chem. Eng. J. 485 (2024) 149779, https://doi.org/10.1016/j.cej.2024.149779.

[5] A. Kostyniuk, B. Likozar, Wet torrefaction of biomass waste into levulinic acid and high-quality hydrochar using H-beta zeolite catalyst, J. Clean. Prod. 449 (2024) 141735, https://doi.org/10.1016/j.jclepro.2024.141735.

[6] A. Kostyniuk, B. Likozar, Wet torrefaction of biomass waste into high quality hydrochar and value-added liquid products using different zeolite catalysts, Renew. Energy 227 (2024) 120509, https://doi.org/10.1016/j.renene.2024.120509.

[7] H. Unyay, P. Piersa, M. Zabochnicka, Z. Romanowska-Duda, P. Kuryło, K. Kuligowski, P. Kazimierski, T. Hutsol, A. Dyjakon, E. Wrzesińska-Jędrusiak, A. Obraniak, S. Szufa, Torrefaction of willow in batch reactor and Co-firing of torrefied willow with coal, Energies 16 (2023) 8083, https://doi.org/10.3390/en16248083.

[8] P. Piersa, S. Szufa, J. Czerwińska, H. Ünyay, Ł. Adrian, G. Wielgosinski, A. Obraniak, W. Lewandowska, M. Marczak-Grzesik, M. Dzikuć, Z. Romanowska-Duda, T.P. Olejnik, Pine wood and sewage sludge torrefaction process for production renewable solid biofuels and biochar as carbon carrier for fertilizers, Energies 14 (2021) 8176, https://doi.org/10.3390/en14238176.

[9] H. Unyay, P. Piersa, N.A. Perendeci, G. Wielgosinski, S. Szufa, Valorization of anaerobic digestate: innovative approaches for sustainable resource management and energy production - case studies from Turkey and Poland, Int. J. Green Energy (2023) 1–16, https://doi.org/10.1080/15435075.2023.2276158.

[10] C. Roos, Biomass drying and dewatering for clean heat & power, North West CHP Appl. Cent. Olympia. (2008).

[11] J. Havlík, T. Dlouhý, Indirect dryers for biomass drying—comparison of experimental characteristics for drum and rotary configurations, ChemEngineering 4 (2020) 1–11, https://doi.org/10.3390/chemengineering4010018.

[12] Z. Romanowska-Duda, K. Piotrowski, S. Szufa, M. Sklodowska, M. Naliwajski, C. Emmanouil, A. Kungolos, A.A. Zorpas, Valorization of Spirodela polyrrhiza biomass for the production of biofuels for distributed energy, Sci. Rep. 13 (2023) 16533, https://doi.org/10.1038/s41598-023-43576-y.

[13] P.L. Simona, P. Spiru, I.V. Ion, Mathematical modelling of sawdust drying process for biomass pelleting, Energy Proc. 141 (2017) 150–154, https://doi.org/10.1016/j.egypro.2017.11.028.

[14] O. Kaplan, C. Celik, An experimental research on woodchip drying using a screw conveyor dryer, Fuel 215 (2018) 468–473, https://doi.org/10.1016/J.FUEL.2017.11.098.

[15] A. Del Giudice, A. Acampora, E. Santangelo, L. Pari, S. Bergonzoli, E. Guerriero, F. Petracchini, M. Torre, V. Paolini, F. Gallucci, Wood chip drying through the using of a mobile rotary dryer, Energies 12 (2019) 1590, https://doi.org/10.3390/en12091590.

[16] H.A. Mohd Yusof, J.L. Ng, S.C. Ng, Y.J. Lee, C.L. Hii, A. Putranto, Modeling of convective drying of sawdust using a reaction engineering approach, Chem. Eng. Technol. 43 (2020) 1802–1812, https://doi.org/10.1002/ceat.202000013.

[17] M. Ozollapins, A. Kakitis, I. Nulle, Stalk biomass drying rate evaluation, Eng. Rural Dev. (2013) 482–487.

[18] J. Yi, X. Li, J. He, X. Duan, Drying efficiency and product quality of biomass drying: a review, Dry. Technol. 38 (2020) 2039–2054, https://doi.org/10.1080/07373937.2019.1628772.

[19] A. Grimm, D. Elustondo, M. Mäkelä, M. Segerström, G. Kalén, L. Fraikin, A. Léonard, S.H. Larsson, Drying recycled fiber rejects in a bench-scale cyclone: influence of device geometry and operational parameters on drying mechanisms, Fuel Process. Technol. 167 (2017) 631–640, https://doi.org/10.1016/J.FUPROC.2017.08.004.

[20] A. Alamia, H. Ström, H. Thunman, Design of an integrated dryer and conveyor belt for woody biofuels, Biomass Bioenergy 77 (2015) 92–109, https://doi.org/10.1016/J.BIOMBIOE.2015.03.022.

[21] H.O.O.K. Of, Arun S. Mujumdar, Handbook of Industrial Drying, Third Edition, 2007, pp. 1–1261, 2007.

[22] M. Intelvi, A. Picado, J. Martínez, Contact Drying Simulation of Particulate Materials : A Comprehensive Approach, vol. 5, 2011, pp. 1669–1676.

[23] W. a Amos, Report on biomass drying technology report on biomass drying technology, SAE Trans. 106 (1998) 475–485.

[24] J. Brammer, A. Bridgwater, Drying technologies for an integrated gasification bio-energy plant, Renew. Sustain. Energy Rev. 3 (1999) 243–289, https://doi.org/10.1016/S1364-0321(99)00008-8.

[25] D.R. Nhuchhen, P. Basu, B. Acharya, Torrefaction of poplar in a continuous two-stage, indirectly heated rotary torrefier, Energy & Fuels 30 (2016) 1027–1038, https://doi.org/10.1021/acs.energyfuels.5b02288.

[26] M. Manouchehrinejad, S. Mani, Process simulation of an integrated biomass torrefaction and pelletization (iBTP) plant to produce solid biofuels, Energy Convers. Manag. X 1 (2019) 100008, https://doi.org/10.1016/j.ecmx.2019.100008.

[27] W.H. Chen, B.J. Lin, Y.Y. Lin, Y.S. Chu, A.T. Ubando, P.L. Show, H.C. Ong, J. S. Chang, S.H. Ho, A.B. Culaba, A. Pétrissans, M. Pétrissans, Progress in biomass torrefaction: principles, applications and challenges, Prog. Energy Combust. Sci. 82 (2021), https://doi.org/10.1016/j.pecs.2020.100887.

[28] Credence Research, Rolling Bed Dryer Market Report No. 23152, 2023.

[29] Allagier, Drying Biomass Rolling Bed Dryer WB-T, 2024.

[30] Mathias Trojosky, Hermann Weiß, Drying of Organic Residuals in the Rolling Bed Dryer, Allgaier Process Technol, GmbH, 2012.

[31] ALMO Process Technology, Low-Temperature Rolling-Bed Dryer, (n.d.).

[32] V. Córdoba, A. Manzur, E. Santalla, Drying kinetics and mathematical modelling of Arundo donax L. canes, a potential renewable fuel, Res. Agric. Eng. 68 (2022) 120–130, https://doi.org/10.17221/73/2021-RAE.

[33] The impact of mechanical pre-treatment of wood biomass on drying rate, Chem. Process Eng. (2023), https://doi.org/10.24425/cpe.2020.132532.

[34] Z. Petrova, Y. Sniezhkin, V. Paziuk, Y. Novikova, A. Petrov, Investigation of the kinetics of the drying process of composite pellets on a convective drying stand, J. Ecol. Eng. 22 (2021) 159–166, https://doi.org/10.12911/22998993/137676.

[35] K. Sacilik, R. Keskin, A.K. Elicin, Mathematical modelling of solar tunnel drying of thin layer organic tomato, J. Food Eng. 73 (2006) 231–238, https://doi.org/10.1016/j.jfoodeng.2005.01.025.

[36] Z. Pakowski, A. Mujumdar, Basic process calculations and simulations in drying, in: Handb. Ind. Drying, third ed., third ed., CRC Press, 2007, pp. 53–80, https://doi.org/10.1201/9781420017618.ch3.

[37] T. Gunhan, V. Demir, E. Hancioglu, A. Hepbasli, Mathematical modelling of drying of bay leaves, Energy Convers. Manag. 46 (2005) 1667–1679, https://doi.org/10.1016/j.enconman.2004.10.001.

[38] C.K.J. Hawlander M. N. A., S.K. Chou, Development of design charts for tunnel dryers, Int. J. Energy Res. 21 (11) (1997) 1023–1037, https://doi.org/10.1002/(SICI)1099-114X(199709)21:113.3.CO, 2-1.

[39] L. Bennamoun, A. Belhamri, Mathematical description of heat and mass transfer during deep bed drying: effect of product shrinkage on bed porosity, Appl. Therm. Eng. 28 (2008) 2236–2244, https://doi.org/10.1016/j.applthermaleng.2008.01.001.

[40] Q. Wang, J. Zhu, T. Li, G. Zhang, Evaluation of the integrated characteristics on combustion and drying using element analysis, Energy & Fuels 28 (2014) 4421–4430, https://doi.org/10.1021/ef5006435.

[41] A. Midilli, H. Kucuk, Mathematical modeling of thin layer drying of pistachio by using solar energy, Energy Convers. Manag. 44 (2003) 1111–1122, https://doi.org/10.1016/S0196-8904(02)00099-7.

[42] R. Stanisławski, Robert Junga, M. Nitsche, Reduction of the CO emission from wood pellet small-scale boiler using model-based control, Energy 243 (2022) 123009, https://doi.org/10.1016/j.energy.2021.123009.

[43] J.L. Parry, Mathematical modelling and computer simulation of heat and mass transfer in agricultural grain drying: a review, J. Agric. Eng. Res. 32 (1985) 1–29, https://doi.org/10.1016/0021-8634(85)90116-7.
[44] J. François, G. Mauviel, M. Feidt, C. Rogaume, Y. Rogaume, O. Mirgaux, F. Patisson, A. Dufour, Modeling of a biomass gasification CHP plant: influence of various parameters on energetic and exergetic efficiencies, Energy & Fuels 27 (2013) 7398–7412, https://doi.org/10.1021/ef4011466.
[45] C. Gustavsson, L. Nilsson, R. Renström, Syngas as an additional energy carrier in the pulp and paper industry: a mill-wide system analysis of a combined drying concept, utilizing on-site generated gas and steam, Energy Fuel. 28 (2014) 5841–5848, https://doi.org/10.1021/ef5010144.
[46] T. Gebreegziabher, A.O. Oyedun, C.W. Hui, Optimum biomass drying for combustion – a modeling approach, Energy 53 (2013) 67–73, https://doi.org/10.1016/J.ENERGY.2013.03.004.
[47] X. He, L. Wang, Experimental determination and modeling of drying process of woody biomass, IOP Conf. Ser. Earth Environ. Sci. 552 (2020) 012016, https://doi.org/10.1088/1755-1315/552/1/012016.
[48] J. Cai, S. Chen, Determination of drying kinetics for biomass by thermogravimetric analysis under nonisothermal condition, Dry. Technol. 26 (2008) 1464–1468, https://doi.org/10.1080/07373930802412116.
[49] J.E. González, B. Coronel Espinoza, V. Quevedo Tumailli, H. Uvidia Cabadiana, D. Oliva M, C.J. Morón, M. Robles Campo, Potential de la biomasa y la cinética del modelo de secado de Piptocoma discolor (pigüe) como fuente de energía renovable en el Ecuador, Enfoque UTE 12 (2021) 74–90, https://doi.org/10.29019/enfoqueute.695.
[50] Q. Xu, S. Pang, Mathematical modeling of rotary drying of woody biomass, dry, Technol. 26 (2008) 1344–1350, https://doi.org/10.1080/07373930802331050.
[51] P. Perré, Multiscale modeling of drying as a powerful extension of the macroscopic approach: application to solid wood and biomass processing, Dry. Technol. 28 (2010) 944–959, https://doi.org/10.1080/07373937.2010.497079.
[52] C. Dupont, R. Chiriac, G. Gauthier, F. Toche, Heat capacity measurements of various biomass types and pyrolysis residues, Fuel 115 (2014) 644–651, https://doi.org/10.1016/j.fuel.2013.07.086.
[53] B. Krupińska, I. Strømmen, Z. Pakowski, T.M. Eikevik, Modeling of sorption isotherms of various kinds of wood at different temperature conditions, dry, Technol. 25 (2007) 1463–1470, https://doi.org/10.1080/07373930701537062.
[54] R.B. Keey, M. Suzuki, On the characteristic drying curve, Int. J. Heat Mass Transf. 17 (1974) 1455–1464, https://doi.org/10.1016/0017-9310(74)90055-6.
[55] B. Krupinska, Model Procesu Suszenia Biomasy Parą Przegrzaną Suszarce Pneuma-Tycznej (A Model of Superheated Steam Drying of Biomass in a Flash Dryer), Łodź University of Technology, 2007.
[56] N. Wakao, S. Kaguei, Heat and Mass Transfer in Packed Beds, ume 1, Gordon and Breach Science Publishers Inc., 1982.
[57] R. Bird, W. Stewart, N. Lightfoot, Transport Phenomena, John Wiley and Sons, New York, 1960, https://doi.org/10.1002/aic.690070245.